Increased sensorimotor structural connectivity in high schizotypy

Eirini Messaritaki[1], Sonya Foley[1], Kali Barawi[2], Ulrich Ettinger[3] and Derek K Jones[1]

1. Cardiff University Brain Research Imaging Centre (CUBRIC), School of Psychology, Cardiff University, Maindy Road, Cardiff, CF24 4HQ, UK
2. School of Medicine, Cardiff University, Cardiff, UK
3. Department of Psychology, University of Bonn, Bonn, Germany

Abstract

We explored the link between brain structural connectivity and schizotypy in healthy participants. Two datasets collected at two different neuroimaging centres, comprising 140 and 115 healthy participants respectively, were used. The participants completed the Schizotypal Personality Questionnaire, through which their total schizotypy scores were calculated. Diffusion MRI data collected at the two centres were used to perform streamline tractography and to generate the structural brain networks of the participants. The edges of the structural networks were weighted with the inverse radial diffusivity. Graph theoretical metrics of the networks were calculated and their correlation coefficients with the schizotypy scores were calculated.

We found a positive correlation between the schizotypy score and both the mean node degree and the mean clustering coefficient of the sensorimotor network. This implies that high-schizotypy participants have stronger connectivity in the sensorimotor network compared to those with low schizotypy. Weaker evidence was found for stronger structural connectivity in high schizotypy in the default-mode and visual networks. Our results agree with the dysconnection hypothesis which suggests that the decreases in white matter structural connectivity observed in schizophrenia patients, rather than being the cause of the disease, could be the result of altered functional connectivity in the disease.

1. Introduction

Schizophrenia is a serious psychiatric disorder of unknown aetiology. Schizotypy encompasses a set of stable personality traits that reflect the subclinical expression of schizophrenia. While individuals with high levels of schizotypy show cognitive and neural patterns resembling the deficits observed in schizophrenia [1, 2], studying schizotypy can also reveal characteristics (in the brain of healthy high-schizotypy participants) which protect or compensate against schizophrenia. Those characteristics may be used to inform the development of novel treatments [1, 2].

The functional brain networks of schizophrenia patients have been shown to be altered compared to healthy participants, and generally exhibit reduced connectivity and less efficient organisation, with few exceptions. For example, a meta-analysis of 13 studies of functional whole-brain networks, in which the functional connectivity was measured via fMRI, magnetoencephalography (MEG) or electroencephalography (EEG), showed significant decreases in small-worldness and in measures of local organisation [3]. Additional studies that were not included in this meta-analysis, corroborate the findings. For example, fMRI-measured functional connectivity was reduced between areas of the default-mode network (DMN) in schizophrenia patients compared to healthy controls [4]. Schizophrenia patients showed reduced activation compared to healthy controls in the lateral frontal cortex bilaterally, in the left basal ganglia and the cerebellum [5]. Those patients and their siblings showed failure of deactivation in the medial frontal cortex compared to healthy controls, with siblings showing less failure than the patients, possibly pointing to DMN dysfunction related to the disease itself [5]. The lateral DMN exhibited decreased fMRI functional connectivity with the unimodal sensorimotor cortex, but increased connectivity with the heteromodal association areas in schizophrenia patients [6]. The anterior and posterior DMNs exhibited increased and decreased connectivity with the right control and lateral visual networks respectively, in schizophrenia patients [6]. Analysis of dynamic fMRI functional connectivity (calculated via a Hidden Markov Model) showed

that schizophrenia patients activated the DMN less frequently than healthy controls, but each activation lasted 4-5 s longer than in the healthy controls [7]. Altered fMRI functional connectivity was observed in the sensorimotor, visual and auditory nodes in schizophrenia patients compared to controls [8], with most of the alterations indicating reduced functional connectivity. Decreased fMRI functional connectivity was observed in schizophrenia patients compared to controls in 26 brain areas related to social, high level cognitive, somatosensory and motor processing [9]. Reduced resting-state functional connectivity (measured with fMRI) was observed in schizophrenia patients compared to controls in the visual and sensorimotor networks [10]. Schizophrenia patients exhibited decreased clustering coefficient, global efficiency and local efficiency, and increased characteristic path length of functional networks [11]. Finally, compared to healthy controls, significant hypoconnectivities were observed between the seed regions and the areas in the auditory network (left insula), core network (right superior temporal cortex), default mode network (right medial prefrontal cortex, and left precuneus and anterior cingulate cortices), self-referential network (right superior temporal cortex), and somatomotor network (right precentral gyrus) in schizophrenia patients [12].

The structural brain networks of schizophrenia patients have predominantly been shown to have a less central and less efficient organisation compared to those of healthy controls, but there are some exceptions. For example, the global efficiency, local efficiency, clustering coefficient, and mean connectivity strength of structural networks weighted by the connectivity probability were significantly lower in schizophrenia patients compared to controls, while the mean betweenness centrality was significantly higher in schizophrenia patients [13]. On the other hand, significantly longer path lengths of frontal and temporal regions were observed in magnetization-transfer weighted structural networks of schizophrenia patients compared to controls, and frontal hubs of patients showed a significant reduction of betweenness centrality [14]. Structural networks of schizophrenia patients with auditory visual hallucinations showed increased characteristic path length compared with those of healthy controls [11].

Additionally, schizophrenia patients have increased radial diffusivity and mean diffusivity in some white matter tracts (left thalamo-occipital tracts, right uncinate fascicle, right middle longitudinal fascicle) compared to healthy controls [15, 16]. Such an increase, although non-specific in principle, can be influenced by decrease in myelination or axonal density [17, 18, 19].

In this study we used tractography-derived structural brain networks to investigate possible differences in the organisation of the brain networks of healthy participants with varying schizotypy scores. Various microstructural metrics, such as the number of reconstructed streamlines or the fractional anisotropy, have been used in past studies to assign connectivity strength to structural network edges [20, 21, 22]. In this study, in order to capture the possible impact of altered myelination or axonal density on the strength of the connections, we used the inverse radial diffusivity to assign edge weights. The aims of the study were to explore whether alterations of white matter connectivity in schizophrenia could also be observed in relation to high schizotypy scores, thereby providing a test of the (dis)connectivity between high schizotypy and full-blown schizophrenia. To do so, we used two different datasets, collected at the Cardiff University Brain Research Imaging Centre (CUBRIC) and at the University of Munich, comprising 140 and 115 participants respectively.

2. Methods

Two datasets were collected at CUBRIC between 2014 and 2016 (Cardiff data), and the University of Munich between 2009 and 2011 (Munich data). The scanners and sequences used were different, and the sensitivity of the data to microstructural parameters is, therefore, different. For that reason, we analysed each dataset separately.

Data collection:

Cardiff data:
140 healthy participants (92 female, 19-55 years old, mean=24.7 years, SD=5.0 years) were recruited in and around Cardiff, UK. All procedures were given ethical approval by the Cardiff University School of Psychology Ethics Committee, and all participants gave written informed consent before taking part. All participants had normal or corrected-to-normal vision and had no history of neurological or neuropsychiatric disorders.

All participants completed the English version of the Schizotypal Personality Questionnaire (SPQ) [23], through which their total schizotypy score was calculated. The questionnaire assessed the following traits: ideas of reference, odd beliefs and magical thinking, unusual perceptual experiences, suspiciousness, excessive social anxiety, no close friends, constricted affect, odd or eccentric behaviour, and odd speech.

MRI was carried out on a GE Signa HDx 3T scanner (GE Healthcare, Milwaukee, WI). T1-weighted structural data were acquired using an axial three-dimensional fast spoiled gradient recalled sequence with the following parameters: TR = 8 ms, TE = 3 ms, TI = 450 ms; flip angle = 20°; voxel size = 1 mm; field of view (FOV) ranging from 256 × 192 × 160 mm^3 to 256 × 256 × 256 mm^3 (anterior-posterior/left-right/superior-inferior). The T1 images were downsampled to 1.5-mm isotropic resolution. Diffusion-weighted MRI data were acquired using a peripherally cardiac-gated sequence with b = 1,200 s/mm^2, TR = 20 s, TE = 90 ms, voxel size 2.4 x 2.4 x 2.4 mm^3, zero slice gap, FOV = 230 mm. Data were acquired along 30 unique and isotropically distributed gradient orientations. Three images with no diffusion weighting were also acquired. The diffusion images were co-registered to the T1-weighted images and corrected for head movement and eddy current distortions. Free-water correction was also performed.

Munich data:
115 healthy participants (55 female, aged 18–50 years, mean age = 27.6 years, SD = 8.0 years) were recruited through advertisements in and around Munich, Germany. All experimental procedures were approved by the research ethics committee of the Faculty of Medicine at the University of Munich, in accordance with the current division of the Declaration of Helsinki. Participants were included after thorough clinical screening and only if they did not meet any of the exclusion criteria: any DSM-IV Axis I disorders, first-grade relatives with psychotic disorders, former or current neurological disorders, current physical conditions, current medication except for contraceptives, uncorrected visual impairments. Further inclusion criteria were age between 18 and 55 and German as a first language. All subjects volunteered to take part in the study, gave written informed consent and received a financial compensation for their participation.

All participants completed the German version [24] of the Schizotypal Personality Questionnaire (SPQ, [23]) to yield their total schizotypy score. For the questionnaire, adequate internal consistency and criterion validity have been demonstrated [25, 26]. In our sample, the SPQ subscales showed acceptable to good reliability (Cronbach's alpha for the total score was 0.882).

High-resolution T1-weighted structural images were acquired on a 3T MAGNETOM Verio scanner (Siemens, Erlangen, Germany) using a 12-channel head matrix Rx-coil. A 3-dimensional MPRAGE sequence was used, with repetition time TR = 2400ms, echo time TE = 3.06 ms, flip angle = 9 degrees with 160 slices, slice thickness = 1.0 mm, voxel size = 1.0 × 1.0 × 1.0 mm, field of view FOV = 256 mm. Diffusion-weighted data were acquired using a diffusion-weighted interleaved spin-echo, echo planar imaging sequence with the following parameters: 25 axial slices; slice thickness = 5.2 mm; TE = 107ms; TR = 5s; gap between slices = 5.2 mm; FOV = 230 mm; matrix = 128 x 128; flip angle = 90; bandwidth = 1395 Hz/Px; voxel size = 1.8 x 1.8 x 5.2 mm. Diffusion gradients were applied in 20 directions with b = 1000 s/mm^2, with each image acquired 3 times. Three images with no diffusion weighting were also acquired.

Tractography:
Probabilistic, anatomically constrained streamline tractography was performed using MRtrix [27], employing the iFOD2 algorithm [28, 29, 30]. The maximum angle between successive steps was 50 degrees, the minimum and maximum streamline lengths were 30mm and 250mm respectively, and the FOD amplitude cut-off was 0.06. Two million streamlines were generated for each participant, with the seed points on the interface between grey matter and white matter. Visual inspection of the tractograms was performed to verify that the white matter was adequately covered.

Parcellation and network construction:
To validate our analysis against the use of different cortical/subcortical parcellations, two atlases were employed to identify the areas of the cerebrum that formed the nodes of the structural brain areas: the AAL atlas [31], which comprises 90 areas, and the Desikan-Killiany atlas [32], which comprises 84 areas. FreeSurfer (http://surfer.nmr.mgh.harvard.edu) was used to parcellate the T1 anatomical scans (recon-all) [33, 34] and the Desikan-Killiany atlas was used to identify the 84 areas of the cerebrum that formed the nodes of the structural brain networks (mri_label2vol and labelconvert of MRtrix [27]). The AAL parcellation was calculated using ExploreDTI 4.8.6 [35]. Each dataset was analysed with both atlas parcellations. However, ExploreDTI failed to give a reliable parcellation for the Munich data, which could be due to the somewhat lower resolution of the diffusion MRI images in that dataset. For that reason, the subsequent analysis for the Munich data was limited to the use of the Desikan-Killiany atlas.

In order to exclude tracts that are not reliable due to having been recovered with a small number of streamlines, we applied a threshold NS_{thr} and excluded edges with fewer than NS_{thr} streamlines. Because that threshold is arbitrary [36], we repeated the analysis for thresholds that resulted to mean network sparsity over participants of as low as 0.25.

Edges that survived thresholding were reweighted with the inverse mean radial diffusivity calculated along the voxels spanning the corresponding white-matter tracts. Networks were constructed for the auditory, sensorimotor, visual and default-mode systems, i.e., for subnetworks that have consistently been shown to be altered in schizophrenia patients compared to controls. Three graph theoretical metrics, namely the mean node degree, mean clustering coefficient and mean nodal strength, were calculated for all networks using the Brain Connectivity Toolbox [37]. In order to identify any metrics that were correlated with each other, correlation coefficients were calculated between graph theoretical metrics for each sub/network. Metrics that exhibited correlation coefficients with absolute values higher than 0.85 were considered highly correlated, and one of the metrics was removed from the analysis.

Statistical analysis:
Correlation coefficients were calculated between the demographic characteristics of the participants, i.e., schizotypy score, age and sex, to verify that those were not correlated with each other.

Partial correlation coefficients and the corresponding *p*-values were calculated between the schizotypy score and the graph theoretical metrics of the participants, correcting for age and sex. Outliers identified with 5 times the mean Cook's distance [38] or higher were removed from the analysis. The resulting *p*-values were corrected for multiple comparisons using the false-discovery-rate algorithm [39], applied over all graph theoretical measures of all subnetworks.

In order to understand whether any corelations between the graph theoretical metrics and the schizotypy score are due to all the nodes of each subnetwork, or whether they are driven by a few specific nodes of it, we calculated the correlation coefficient between the schizotypy score and the node-specific graph theoretical metrics, for the graph theoretical metrics that exhibited statistically significant correlations.

The analysis pipeline is shown in Fig. 1.

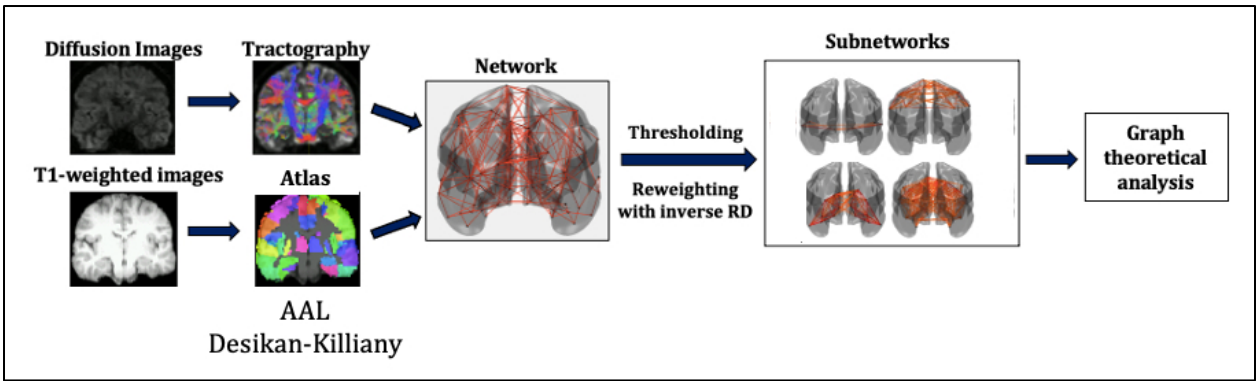

Fig. 1: Analysis pipeline.

3. Results

Demographic information:

The schizotypy scores of the participants in the Cardiff data ranged between 0 and 43 (mean: 24.6, SD: 5.0), while for the Munich data they ranged between 0 and 35 (mean: 8.2, SD: 7.0). No statistically significant correlations were found between schizotypy score and age or sex, or between age and sex of the participants, for the Cardiff or the Munich data. The correlation coefficients and *p*-values between these variables are given in Table 1 for the two datasets.

	Sz score vs. Age	**Sz score vs. Sex**	**Age vs. Sex**
Cardiff data	0.046 (*0.593*)	-0.098 (*0.247*)	-0.067 (*0.430*)
Munich data	-0.14 (*0.146*)	0.17 (*0.057*)	-0.10 (*0.286*)

Table 1: Correlation coefficients and *p*-values (the latter in parentheses) between the demographic data in the two datasets.

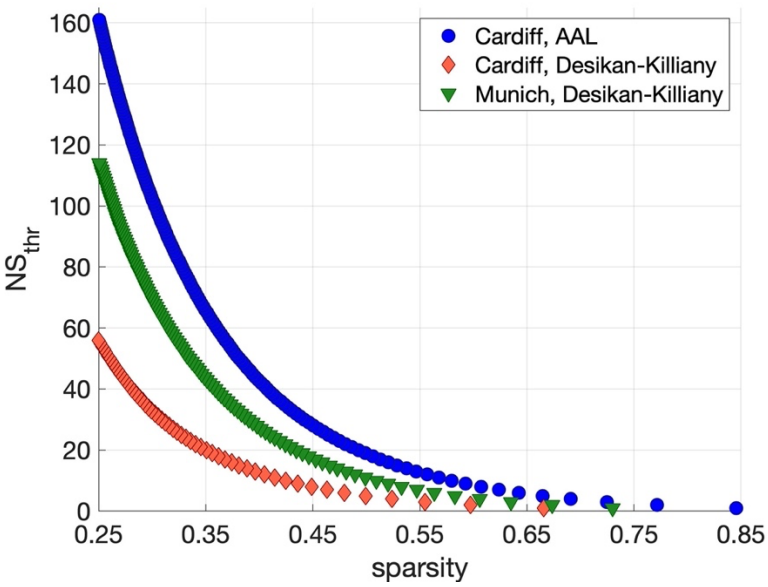

Fig. 2: NS_{thr} required to achieve a given sparsity in the whole-brain structural networks, for the three dataset-atlas combinations.

Network analysis:
The NS_{thr} required to achieve a given group-mean sparsity for the whole-brain network in the three cases investigated is shown in Fig. 2. In order to ensure that we go to sparsities as low at 0.25, we use NS_{thr} of [0, 160] for the Cardiff data / AAL atlas pair, [0, 60] for the Cardiff data / Desikan-Killiany pair, and [0, 120] for the Munich data / Desikan-Killiany pair.

Cardiff data, AAL atlas:
Statistically significant positive correlations that survived multiple comparison correction and persisted across NS_{thr} were identified between schizotypy score and the mean node degree, and between schizotypy score and the mean clustering coefficient, for the sensorimotor network. The correlation coefficients and *p*-values across NS_{thr} are shown in Fig. 3. In that figure, the bold colors indicate the correlation coefficients and *p*-values that survived multiple-comparison correction, while the faded colors indicate correlations that were nominally statistically significant ($p<0.05$) but did not survive multiple comparison correction. A statistically significant positive correlation between the schizotypy score and the mean node degree of the default-mode network was also found for the higher NS thresholds. Scatter plots for these correlations are shown in Fig. 4.

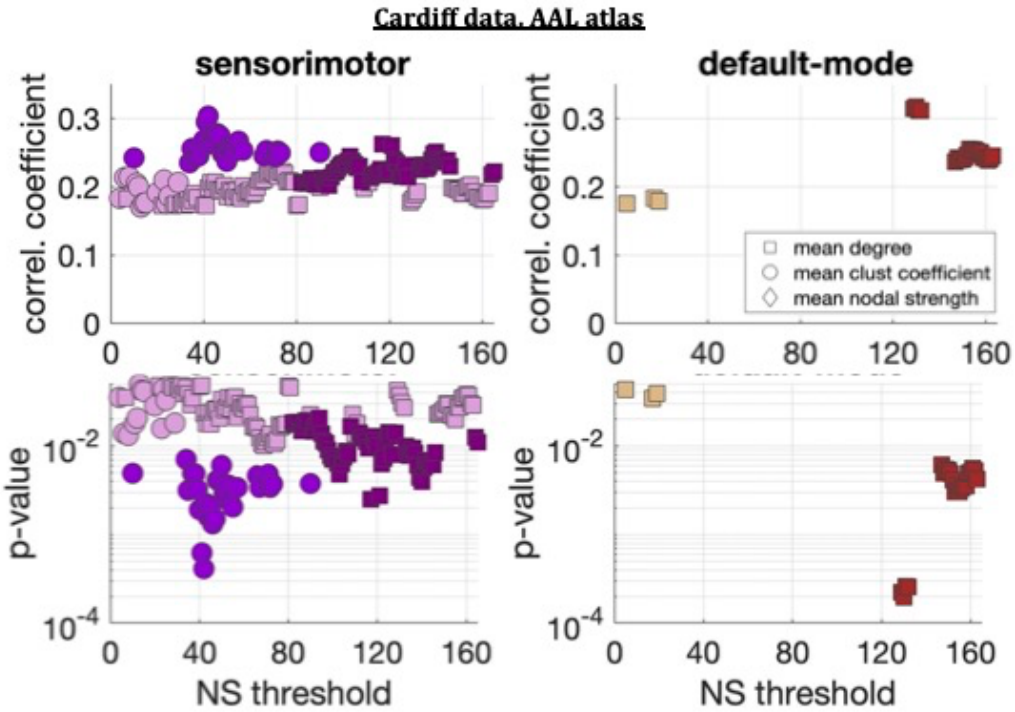

Fig. 3: Correlation coefficients and p-values between graph theoretical metrics and schizotypy score for the Cardiff data and the AAL atlas. Only the two subnetworks that show persistent correlations across thresholds are shown.

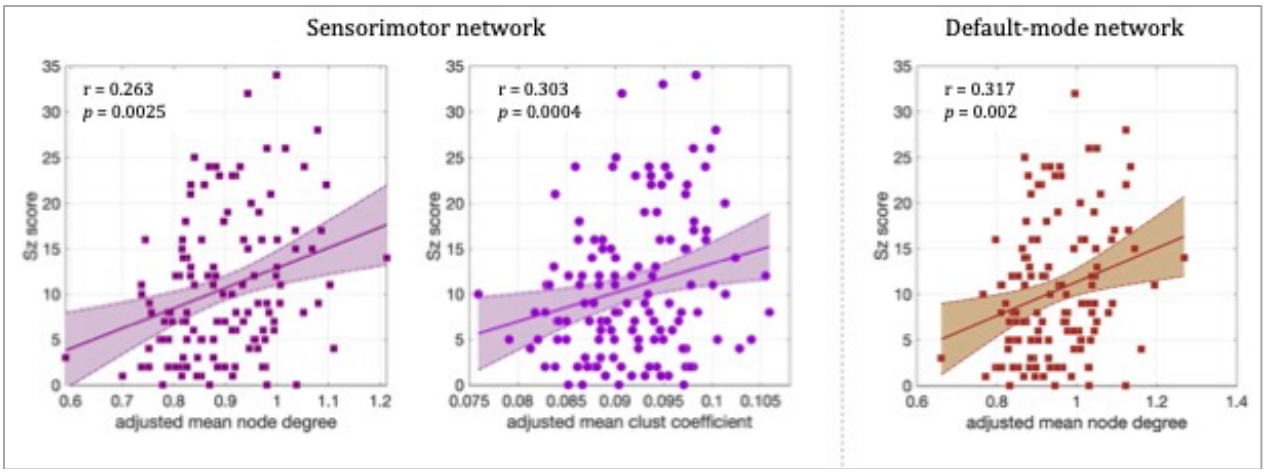

Fig. 4: Scatter plots for the correlations observed in the Cardiff data for the AAL atlas parcellation.

Cardiff data, Desikan-Killiany atlas:
Statistically significant positive correlations were identified between schizotypy score and the mean node degree of the sensorimotor network, shown in Fig. 5. These survived multiple comparison correction for NS thresholds in the range of 35 to 45 but were persistent across NS thresholds. The corresponding scatter plots are shown in Fig. 6.

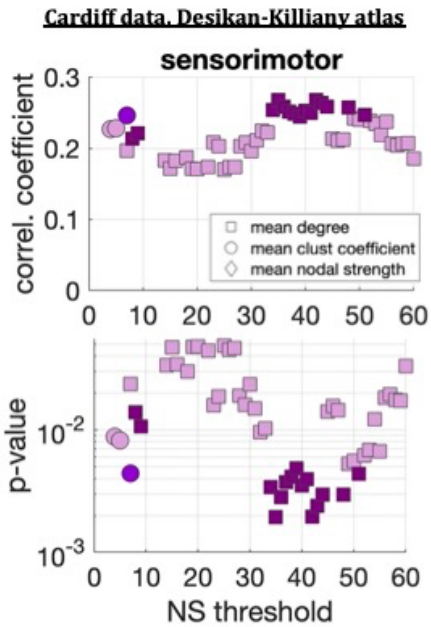

Fig. 5: Correlation coefficients and p-values between graph theoretical metrics and schizotypy score for the Cardiff data and the Desikan-Killiany atlas. Only the sensorimotor subnetwork showed persistent correlations across thresholds.

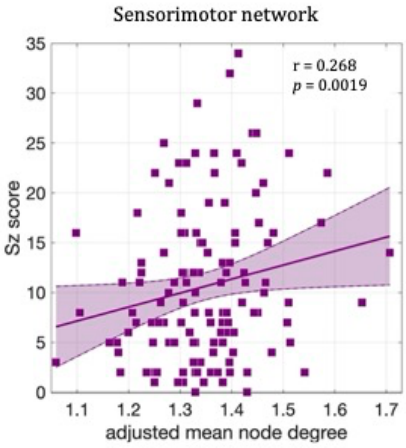

Fig. 6: Scatter plots for the correlations observed in the Cardiff data for the Desikan-Killiany parcellation.

Munich data, Desikan-Killiany atlas:
Statistically significant positive correlations between the schizotypy score and the mean node degree of the sensorimotor network were identified (Fig. 7). They were nominally statistically significant but persisted across NS thresholds. Similarly, nominally statistically significant correlations were identified between the mean node degree and the schizotypy score for the visual network across the lower NS thresholds that we considered for this dataset/atlas pair. The corresponding scatter plots are shown in Fig. 8.

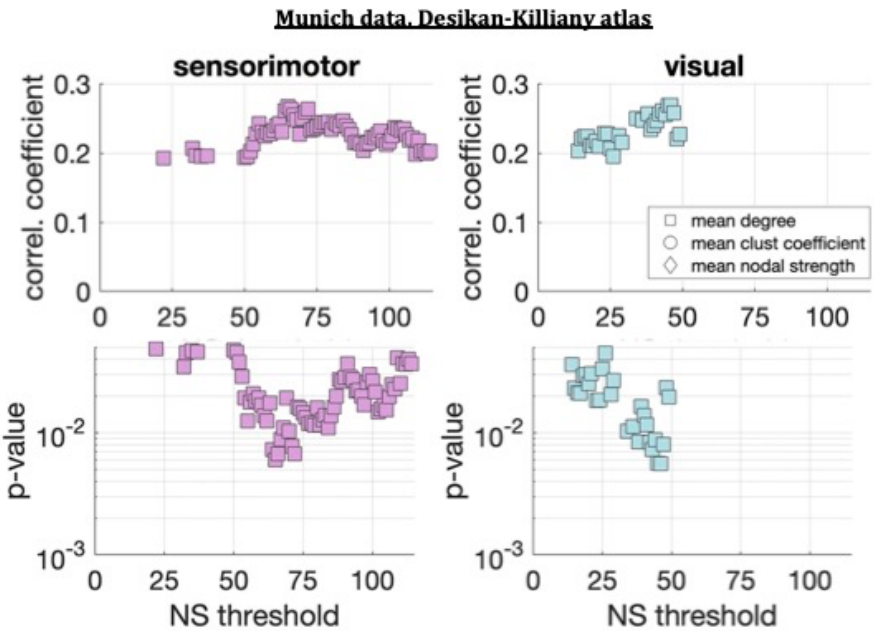

Fig. 7: Correlation coefficients and p-values between graph theoretical metrics and schizotypy score for the Munich data and the Desikan-Killiany atlas. Only the sensorimotor and the visual subnetworks showed persistent correlations across thresholds, and those were nominally statistically significant.

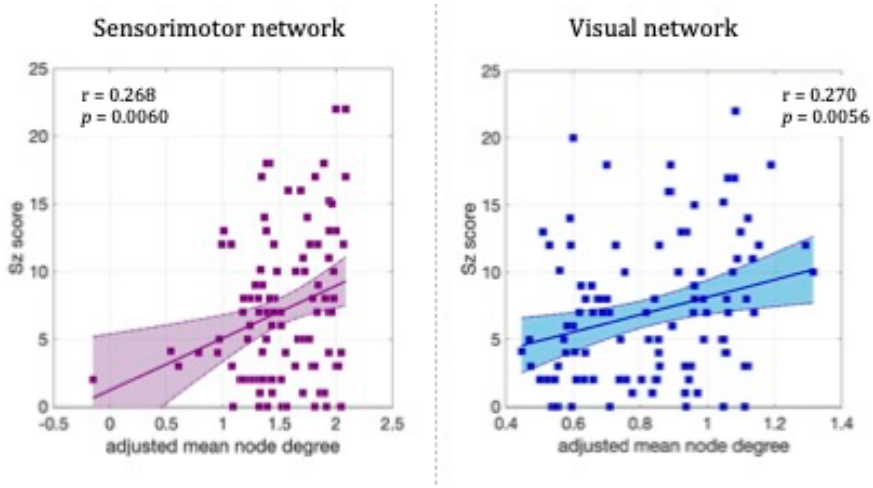

Fig. 8: Scatter plots for the correlations observed in the Munich data for the Desikan-Killiany parcellation.

<u>Node-specific analysis:</u>
The node-specific analysis was limited to the sensorimotor network because that was the one whose mean node degree showed consistent correlations with the schizotypy score across the two datasets and atlases and across NS thresholds.

Cardiff data, AAL atlas:
The node-specific analysis for the sensorimotor network showed that the correlations between the schizotypy score and the mean node degree are driven by the right precental gyrus, the right supramarginal gyrus, the right paracentral lobule and the right middle frontal gyrus. The correlations between the schizotypy score and the mean clustering coefficient are driven by the right precentral gyrus, the right supplementary motor area, the left and right postcentral gyrus and the left paracentral lobule. The correlation coefficients and respective *p*-values are shown in Table 2.

Cardiff data, Desikan-Killiany atlas:
The node-specific analysis showed that the correlations between the schizotypy score and the mean node degree of the sensorimotor network were driven by the left and right paracental lobule, the left and right supramarginal gyrus, the right precentral gyrus, the right caudal middle frontal gyrus and the left superior frontal gyrus (correlation coefficients and *p*-values shown in Table 2).

Munich data, Desikan-Killiany atlas:
The node-specific analysis showed that the correlations between schizotypy score and the mean node degree of the sensorimotor network were driven by the left paracentral lobule, the left supramarginal gyrus the left and right precentral gyrus and the left and right postcentral gyrus (correlation coefficients and *p*-values shown in Table 2).

Dataset / Atlas	**Metric**	**Brain area**	**correlation coefficient (r)**	***p*-value**
Cardiff data AAL atlas	**mean degree**	R precentral gyrus	0.18	0.0442
		R supramarginal gyrus	0.18	0.0336
		R paracentral lobule	0.18	0.0393
		R middle frontal gyrus	0.19	0.0278
	mean clustering coefficient	R precentral gyrus	0.28	0.0013
		R supplementary motor area	0.20	0.0220
		L postcentral gyrus	0.18	0.0352
		R postcentral gyrus	0.22	0.0117
		L paracentral lobule	0.20	0.0252
Cardiff data	**mean**	L paracentral lobule	0.24	0.0067

Desikan-Killiany atlas	**degree**	L postcentral gyrus	0.19	0.0349
		R caudal middle frontal gyrus	0.19	0.0306
		R superior frontal gyrus	0.20	0.0263
Munich data **Desikan-Killiany atlas**	**mean degree**	L precentral gyrus	0.22	0.0225
		R precentral gyrus	0.22	0.0242
		L supramarginal gyrus	0.26	0.0080
		L paracentral lobule	0.38	0.0001
		L postcentral gyrus	0.20	0.0430
		R postcentral gyrus	0.31	0.0015

Table 2: Correlation coefficients and *p*-values between schizotypy score and the node degree of the nodes of the sensorimotor network that drive the correlations.

4. Discussion

We investigated the graph theoretical properties of the structural brain networks of healthy participants with a range of schizotypy scores. To the best of our knowledge, this is the first time these properties are investigated in relation to schizotypy. We used two large datasets, comprising 140 and 115 participants respectively, collected at different MRI scanners and with different scanning parameters.

Our results provide evidence that high-schizotypy healthy participants have higher structural connectivity in the sensorimotor network, with some increases also possibly present in the default-mode and visual networks. The edges of the networks were weighted by the inverse radial diffusivity, which partly reflects differences in myelination or axon density [17, 18]. Both myelination and axon density support effective communication in the brain [40, 41].

A recent study [42] showed that high schizotypy participants exhibited increased white matter connectivity probability (measured via the number of water molecules passing through the brain areas, divided by the total number of streamlines generated from those brain areas) between the right middle frontal gyrus and the right insula. Increased strength values were found between the left superior frontal gyrus and the right rolandic operculum area, and between the right superior frontal gyrus and the right medial superior frontal gyrus. This pattern of stronger structural connectivity is in agreement with our results. The same study also showed that this enhanced structural connectivity appears along decreases in functional connectivity in the sensorimotor network in the higher schizotypy participants. While the general pattern of stronger white-matter connectivity in relation to higher schizotypy agrees with our finding, we note that differences between studies include that their study had participants with many schizotypy scores higher than the ones in our study, they did not use graph theory in their analysis, and their connectivity measure is more closely related to the number of streamlines rather than to the myelination or axonal density in the white matter tracts that we used.

As mentioned in the Introduction, a pattern of decreased functional connectivity has been consistently reported in the literature for schizophrenia patients compared to healthy controls. Structural connectivity has also been observed to be reduced in schizophrenia, although the findings are less coherent, most likely due to differences in the analysis pipelines used. In this context, there are two possible interpretations for our results.

The first interpretation is that our results support the notion that increased structural connectivity in the sensorimotor network of healthy high-schizotypy participants could be enhancing communication among sensorimotor regions, i.e., regions implicated in action observation and imitation [43], which are functions crucial for successful social interactions. This enhanced communication could be protecting these participants from the development of schizophrenia. This interpretation also indicates that structural deficiencies in the sensorimotor network should be further investigated as causes of schizophrenia.

Another possible interpretation is that the white matter structural alterations that have been reported in schizophrenia patients [11, 13, 14, 15, 16], may be the pathophysiological consequence or correlate of worsening schizophrenia symptoms, particularly in chronic schizophrenia, rather than the cause of the disease. This is in agreement with the dysconnection hypothesis [44]. We also note that schizophrenia is normally diagnosed in the late teens to early 20s in men and in the late 20s to early 30s in women. This observation points to this latter interpretation being more likely for our results. This is because many of the participants in both samples were under 30 years old at the time that the studies were run. Therefore, some of the high-schizotypy participants in our samples could, at some time after the study, develop schizophrenia, which would indicate that the increased structural connectivity in the sensorimotor network could not protect them from developing the disease.

Our findings relating to which nodes of the sensorimotor network drive the increase in its structural connectivity can also be put in the context of findings in the literature. These nodes have predominantly been shown to have reduced functional connectivity in schizophrenia patients compared to healthy controls. For example, the left and right postcentral gyri were shown to have reduced functional connectivity between them [8]. The postcentral gyrus was shown to have reduced grey matter density in schizophrenia patients [45], and its reduced connectivity has been shown to have a central role in early-onset schizophrenia [46]. The global-brain functional connectivity of the left precentral and postcentral gyri was lower in adolescent-onset schizophrenia patients compared to controls, although it was increased in the right middle frontal gyrus [47]. The right precentral gyrus was shown to have hypoconnectivity in schizophrenia patients compared to controls [12]. The left paracentral lobule and the right precentral gyrus were shown to have lower regional homogeneity, a quantity that reflects local functional connectivity and regional integration of information processing [48], in adolescent-onset schizophrenia patients.

These decreases in connectivity in schizophrenia patients, put together with the increases in structural connectivity in the same nodes in the healthy participants of higher schizotypy, further corroborate the two possible explanations that we provided for our results.

A strength of our study stems from the fact that we used two large datasets, comprising 140 and 115 participants. Despite the differences in scanners and scanning sequences, the findings of stronger connectivity in the sensorimotor network were replicated in the two datasets, and employing two different atlases for brain parcellation. Our tractography generation is state-of-the-art, utilising an algorithm that limits the presence of false positive tracts. Using the inverse radial diffusivity to assign strength to the structural connections relates them to the myelination or the axonal density of the white matter tracts, which are measures that better reflect efficient brain communication than the more frequently used number of streamlines or fractional anisotropy [21]. One limitation of our study is the fact that the schizotypy scores went only up to 43, when the maximum possible value is 74. This is a typical range for schizotypy studies but indicates that our results should be interpreted for healthy participants with schizotypy scores in the corresponding range. In the future, diffusion MRI studies should employ higher b-values than those used in this study, in order to provide enhanced sensitivity to myelination and axonal diameter of the white matter tracts, and to allow us to further investigate structural connectivity in high schizotypy.

5. Conclusions

We investigated the graph theoretical properties of structural brain subnetworks in healthy participants of varying schizotypy scores. We identified an increase in the structural connectivity of the sensorimotor network in participants with high schizotypy score. This can indicate a possible protective mechanism against schizophrenia or could be another consequence of the dysconnection that has been hypothesized to be the underlying cause of schizophrenia. Our results, therefore, support existing hypotheses about the potential origins of schizophrenia and suggest possible treatment targets to be explored.

Acknowledgements
EM was funded by a Wellcome Trust ISSF Postdoctoral Research Fellowship at Cardiff University (204824/Z/16/Z). DKJ was funded by a Wellcome Trust Investigator Award (096646/Z/11/Z) and a Wellcome Trust Strategic Award (104943/Z/14/Z). SF was funded on an Institutional Strategic Support Fund Grant No. 504182 awarded to Cardiff University by the Wellcome Trust. UE acknowledges funding from the Deutsche Forschungsgemeinschaft (ET 31/2-1).

References:
1. U. Ettinger, C. Mohr, D. C. Gooding, A. S. Cohen, A. Rapp, C. Haenschel, S. Park. Cognition and brain function in Schizotypy: a selective review. (2015) *Schizophrenia Bulletin*, 41:S417-S426.
2. U. Ettinger. I. Meyhöfer, M. Steffens, M. Wagner, N. Koutsouleris. Genetics, cognition, and neurobiology of schizotypal personality: a review of the overlap with schizophrenia. (2014) *Frontiers in Psychiatry*, 5:18.
3. J. Kambeitz, L. Kambeitz-Ilankovic, C. Cabral, D. B. Dwyer, V. D. Calhoun, M. P. van den Heuvel, P. Falkai, N. Koutsouleris, B. Malchow. Aberrant functional whole-brain network architecture in patients with schizophrenia: a meta-analysis. (2016) *Schizophrenia Bulletin*, 42:S13-S21.
4. A. Pankow, L. Deserno, M. Walter, T. Fydrich, F. Bermpohl, F. Schlagenhauf, A. Heinz. Reduced default mode network connectivity in schizophrenia patients. (2015) *Schizophrenia Research*, 165(1):90-93.
5. R. Landin-Romero, P. J. McKenna, P. Salgado-Pineda, S. Sarró, C. Aquirre, C. Sarri, A. Compte, C. Bosque, J. Blanch, R. Salvador, E. Pomarol-Clotet. Failure of deactivation in the default mode network: a trait marker of schizophrenia? (2014) *Psychological Medicine*, 45(6):1315-1325.
6. H. Wang, L.-L. Zeng, Y. Chen, H. Yin, Q. Tan, D. Hu. Evidence of a dissociation pattern in default mode subnetwork functional connectivity in schizophrenia. (2015) *Scientific Reports*, 5:14655.
7. A. Kottaram, L. A. Johnston, L. Cocchi, E. P. Ganella, I. Everall, C. Pantelis, R. Kotagiri, A. Zalesky. Brain network dynamics in schizophrenia: reduced dynamism of the default mode network. (2019) *Human Brain Mapping*, 40:2212-2228.
8. T. Kaufmann, K. C. Skåtun, D. Alnæs, N. T. Doan, E. P. Duff, S. Tønnesen, E. Roussos, T. Ueland, S. R. Aminoff, T. V. Lagerberg, I. Agartz, I. S. Melle, S. M. Smith, O. A. Andreassen, L. T. Westlye. Disintegration of sensorimotor brain networks in schizophrenia. (2015), *Schizophrenia Bulletin*, 41(6): 1326-1335.
9. R. A. Berman, S. J. Gotts, H. M. McAdams, D. Greenstein, F. Lalonde, L. Clasen, R. E. Watsky, L. Shora, A. E. Ordonez, A. Raznahan, A. Martin, N. Gogtay, J. Rapoport. Disrupted sensorimotor and social-cognitive networks underlie symptoms in childhood-onset schizophrenia. (2016) *Brain*, 139(1): 276-291.
10. A. M. Jimenez, P. Riedel, J. Lee, E. A. Reavis, M. F. Green. Linking resting-state networks and social cognition in schizophrenia and bipolar disorder. (2019) *Human Brain Mapping*, 40:4703-4715.
11. J. Zhu, C. Wang, F. Liu W. Qin, J. Li and C. Zhuo. Alterations of functional and structural networks in schizophrenia patients with auditory verbal hallucinations. (2016) *Front Hum Neurosci*., 10, DOI=10.3389/fnhum.2016.00114
12. S. Li, N. Hu, W. Zhang, B. Tao, J. Dai, Y. Gong, Y. Tan, D. Cai, S. Lui. Dysconnectivity of multiple brain networks in schizophrenia: a meta-analysis of resting-state functional connectivity. (2019) *Frontiers in Psychiatry*, 10:482.
13. S.-H. Shon, W. Yoon, H. Kim, S. W. Joo, Y. Kim and J. Lee. Deterioration in global organisation of structural brain networks in schizophrenia: a diffusion MRI tractography study. (2018) *Front Psychiatry* doi.org/10.3389/fpsyt.2018.00272
14. M. P. van den Heuvel, R. C. W. Mandl, C. J. Stam, R. S. Kahn, H. E. Hulshoff Pol. Aberrant frontal and temporal complex network structure in schizophrenia: a graph theoretical analysis. (2010) *J. Neurosci*, 30(47):15915-15926.
15. S. W. Joo, W. Yoon, S.-H. Shon, H. Kim, S. Cha, K. J. Park and L. Lee. Altered white matter connectivity in patients with schizophrenia: An investigation using public neuroimaging data from SchizConnect. (2018) *PLoS One*, 13(10), e0205369.

16. M. F. Abdul-Rahman, A. Qiu and K. Sim. Regionally specific white matter disruptions of fornix and cingulum in schizophrenia. (2011) *PLoS One*, 6(4):e18652.
17. Y. Chen, H. An, H. Zhu, T. Stone, J. K. Smith, C. Hall, E. Bullitt, D. Shen, W. Lin. White matter abnormalities revealed by diffusion tensor imaging in non-demented and demented HIV+ patients. (2009) *NeuroImage*, 47:1154–1162
18. M. D. Cykowski, P. T. Fox, R. J. Ingham, J. C. Ingham, D. A. Robin. A study of the reproducibility and etiology of diffusion anisotropy differences in developmental stuttering: a potential role for impaired myelination. (2010) *NeuroImage*, 52:1495–1504.
19. D. K. Jones, T. R. Knösche and R. Turner. White matter integrity, fiber count and other fallacies: the do's and dont's of diffusion MRI. (2013) *NeuroImage*, 73:239-254.
20. K. Caeyenberghs, C. Metzler-Baddeley, S. Foley, D.K. Jones. Dynamics of the human structural connectome underlying working memory training, (2016) *J. Neurosci.*, 36 (14):4056-4066.
21. E. Messaritaki, S. Foley, S. Schiavi, L Magazzini, B. Routley, D. K. Jones and K. D. Singh. Predicting MEG resting-state functional connectivity from microstructural information. (2021) *Network Neuroscience*, 5(2):477-504.
22. E. Messaritaki, S. I. Dimitriadis, D. K. Jones. Optimization of graph construction can significantly increase the power of structural brain network studies. (2019) *NeuroImage*, 199:499-511.
23. A. Raine. The SPQ: a scale for the assessment of schizotypal personality based on DSM-III-R criteria. (1991) *Schizophrenia Bulletin* 17, 555–564.
24. C. Klein, B. Andresen and T. Jahn. Erfassung der schizotypen persönlichkeit nach DSM-II-R: psychometrische eigenschaften einer autorisierten deutschsprachigen Übersetzung des 'Schizotypal Personality Questionnaire' (SPQ) von Raine. (1997) *Diagnostica* 43, 347–369.
25. C. Klein, B. Andresen and T. Jahn. Konstruktvalidierung der deutschsprachigen adaptation des Schizotypal Personality Questionnaires (SPQ) von Raine (1991). In Andresen, B and Maß, R (eds). (2001) *Schizotypie. Psychometrische Entwicklungen und Biopsychologische Forschungsansätze. Göttingen: Hogrefe*, pp. 349–378
26. E. Fonseca-Pedrero, J. Ortuño-Sierra, B. Lucas-Molina, M. Debbané, R. C. K. Chan, D. C. Cicero, L. C. Zhang, C. Brenner, E. Barkus, R. J. Linscott, T. Kwapil, N. Barrantes-Vidal, A. Cohen, A. Raine, M. T. Compton, E. B. Tone, J. Suhr, J. Bobes, A. Fumero, S. Giakoumaki, I. Tsaousis, A. Preti, M. Chmielewski, J. Laloyaux, A. Lechri, M. A. Lahmar, V. Wuthrich, F. Larøi, J. C. Badcock, A. Jablensky, D. Barron, V. Swami, U. S. Tran, and M. Voracek. Brief assessment of schizotypal traits: a multinational study. (2018) *Schizophrenia Research* 197, 182–191.
27. J.-D. Tournier, R. E. Smith, D. Raffelt, R. Tabbara, T. Dhollander, M. Pietsch, D. Christiaens, B. Jeurissen, C.-H. Yeh, A. Connelly. MRtrix3: A fast, flexible and open software framework for medical image processing and visualisation. (2019) *NeuroImage*, 202:116-37.
28. J.-D. Tournier, F. Calamante and A. Connelly. Improved probabilistic streamlines tractography by 2nd order integration over fibre orientation distributions. (2010) *Proceedings of the International Society for Magnetic Resonance in Medicine*, 1670.
29. R. E. Smith, J.-D. Tournier, F. Calamante, A. Connelly. Anatomically-constrained tractography: Improved diffusion MRI streamlines tractography through effective use of anatomical information. (2012) *NeuroImage*, 62:1924-1938.
30. R. E. Smith, J.-D. Tournier, F. Calamante, A. Connelly. SIFT2: Enabling dense quantitative assessment of brain white matter connectivity using streamlines tractography. NeuroImage, 2015, 119, 338-351
31. N. Tzourio-Mazoyer, B. Landeau, D. Papathanassiou, F. Crivello, O. Etard, N. Delcroix, B. Mazoyer, M. Joliot. Automated anatomical labeling of activations in SPM using a macroscopic anatomical parcellation of the MNI MRI single-subject brain. (2002) *NeuroImage*, 15(1):273-289.
32. R. S. Desikan, F. Segonne, B. Fischl, B. T. Quinn, B. C. Dickerson, D. Blacker, R. L. Buckner, A. M. Dale, R. P. Maquire, B. T. Hyman, M. S. Albert and R. J. Killiany. An automated labeling system for subdividing the human cerebral cortex on MRI scans into gyral based regions of interest. (2006) *NeuroImage*(31): 968-980.
33. B. Fischl, D. H. Salat, E. Busa, M. Albert, M. Dieterich, C. Haselgrove, A. van der Kouwe, R. Killiany, D. Kennedy, S. Klaveness, A. Montilo, N. Makris, B. Rosen, A. M. Dale. Whole brain segmentation: Automated labeling of neuroanatomical structures in the human brain. (2002) *Neuron*, 33, 341– 355.

34. B. Fischl, D. H. Salat, A. J. W. van der Kouwe, N. Makris, F. Ségonne, B. T. Quinn, A. M. Dale. Sequence-independent segmentation of magnetic resonance images. (2004) *NeuroImage*, 23(Supplement 1), S69– S84
35. A. Leemans, B. Jeurissen, J. Sijbers, D. K. Jones. "ExploreDTI: A graphical toolbox for processing, analyzing, and visualizing diffusion MR data". Proceedings of the 17th Scientific Meeting, International Society for Magnetic Resonance in Medicine, Honolulu, USA, p. 3537, 2009.
36. C. R. Buchanan, M. E. Bastin, S. J. Ritchie, D. C. Liewald, J. W. Madole, E. M. Tucker-Drob, I. J. Deary, S. R. Cox. The effect of network thresholding and weighting on structural brain networks in the UK Biobank. (2020) *NeuroImage*, 211:116443.
37. M. Rubinov and O. Sporns. Complex network measures of brain connectivity: uses and interpretations. (2010) *NeuroImage*. 52(3): 1059-1069.
38. R. D. Cook. Detection of influential observations in linear regression. (1977) Technometrics, 19(1):15-18.
39. Y. Benjamini and D. Yekutieli. The control of the false discovery rate in multiple testing under dependency. (2001) *The Annals of Statistics*, 29(4): 1165-1188.
40. M. Drakesmith, R. Harms, S. U. Rudrapatna, G. D. Parker, C. J. Evans and D. K. Jones. Estimating axon conduction velocity in vivo from microstructural MRI. (2019) *NeuroImage*, 203:116186.
41. C. Lebel and S. Deoni. The development of brain white matter microstructure. (2018) *NeuroImage*, 182:207-218.
42. Y.-M. Wang, X.-L. Cai, R.-T. Zhang, Y.-J. Zhang, H.-Y. Zhou, Y. Wang, Y. Wang, J. Huang, Y.-Y. Wang, E. F. C. Cheung, R. C. K. Chan. Altered brain structural and functional connectivity in schizotypy. (2020) *Psychological Medicine*, 1-10.
43. S. Caspers, K. Zilles, A. R. Laird, S. B. Eickhoff. ALE meta-analysis of action observation and imitation in the human brain. (2010) *NeuroImage*, 50(3):1148–1167.
44. K. Friston, H. R. Brown, J. Siemerkus and K. E. Stephan. The dysconnection hypothesis (2016). (2016) Schizophrenia Research, 176(2-3): 83-94.
45. D. C. Glahn, A. R. Laird, I. Ellison-Wright, S. M. Thelen, J. L. Robinson, J. L. Lancaster, E. Bullmore, P. T. Fox. Meta-analysis of grey matter anomalies in schizophrenia: application of anatomic likelihood estimation and network analysis. (2008) *Biol Psychiatry*, 64: 774– 781.
46. H. J. Li, Y. Xu, K. R. Zhang, M. J. Hoptman, X. N. Zuo. Homotopic connectivity in drug-naive, first-episode, early-onset schizophrenia. (2015) *J Child Psychol Psychiatry*. 2014;56:432–443.
47. J. Zhao, Y. Zhang, F. Liu, J. Chen, J. Zhao, W. Guo. Abnormal global-brain functional connectivity and its relationship with cognitive deficits in drug-naive first-episode adolescent-onset schizophrenia. (2022), *Brain Imaging and Behavior*, doi.org/10.1007/s11682-021-00597-3.
48. S. Wang, Y. Zhang, L. Lv, R. Wu, X. Fan, J. Zhao, W. Guo. Abnormal regional homogeneity as a potential imaging biomarker for adolescent-onset schizophrenia: A resting-state fMRI study and support vector machine analysis. (2018), *Schizophrenia Research*, 192:179-184.